



X International Conference on Structural Dynamics, EURODYN 2017

## Extraction of damage-sensitive eigen-parameters for supervised SHM

Maria Giovanna Masciotta<sup>a,\*</sup>, Luís F. Ramos<sup>a</sup>, Marcello Vasta<sup>b</sup>, Paulo B. Lourenço<sup>a</sup>

<sup>a</sup>ISISE, University of Minho, Department of Civil Engineering, Campus de Azurém, 4800-058, Guimarães, Portugal  
<sup>b</sup>University "G. d'Annunzio, Department of Engineering and of Geology, Viale Pindaro, 65127, Pescara, Italy

---

### Abstract

These last decades have seen an exponential increase in the amount of research related to structural health monitoring (SHM) due to its potential for significant life-safety and economic benefits. However, the success of this powerful tool strongly depends on the implemented damage identification strategy. Reliable and efficient damage identification algorithms enable to detect faults that lie beneath the surface of the structure and to spot system's vulnerabilities at a very early-stage. This allows to adopt appropriate remedial measures in a timely fashion thereby minimizing the risk of unexpected collapses.

The present paper describes a spectrum-driven damage identification method that investigates three levels of damage, i.e. detection, localisation and assessment. Peculiarity of the method is the use of spectral frequency-dependent Eigen-parameters estimated from the response Power Spectral Density (PSD) matrix, which is demonstrated to be very sensitive to damage-induced changes. The approach is detailed, including initial assumptions, scientific formulation of the problem and derivation of the algorithm. Finally, the effectiveness of the method is validated through a numerical simulation and verified on a case-study structure.

© 2017 The Authors. Published by Elsevier Ltd.

Peer-review under responsibility of the organizing committee of EURODYN 2017.

**Keywords:** Structural health monitoring; dynamic identification; damage-sensitive eigen-parameters; power spectral densities; damage localisation.

---

---

\* Corresponding author. Tel.: +351 917 099 832; fax: +351 253 510 217.

E-mail address: [mg.masciotta@gmail.com](mailto:mg.masciotta@gmail.com)

## 1. Introduction

Built environment is continuously exposed to the risk of damage, whether due to exogenous or endogenous causes. If not timely identified, damage can compromise the structural performance of the affected system, causing an impairment of its normal function until structural soundness is restored. To avoid that, damage should be located at a very early stage so as to design in advance adequate retrofit solutions while keeping on ensuring users' safety throughout the structure lifespan. Hitherto, vibration-based damage identification methods (VBDIMs) have proven to be the best tool available for the structural assessment of engineering systems [1-3] and heritage buildings, allowing the identification of the most vulnerable areas without jeopardizing the original construction. Being global methods, VBDIMs are also worth to be used as tools for primary inspection in order to detect damaged areas and better address local methods, which would be rather time-consuming to apply without any previous knowledge about the damage position. Over the past decades, several damage identification methods have been proposed in literature [4-6]. However, to the knowledge of the authors, none of the methods currently available seems to be efficient for all structural typologies. The present paper attempts to provide a valid contribution to this field by presenting a spectrum-driven approach for early-stage damage identification, whose formulation can be extended beyond civil engineering applications.

## 2. Spectrum-driven method for damage identification

### 2.1. Initial assumptions and formulation of the problem

In stochastic environment, the dynamic characterization of a given structural system can be performed through the application of normal spectral analysis methods. Because of their explicit dependence on the frequency content, power spectral densities are very sensitive to variations of stiffness caused by evolutionary damage scenarios [7]. This means that system's structural changes are reflected by changes in its spectral response, thus the occurrence of damage can be detected by analyzing the eigen-parameters extracted from the decomposition of the response Power Spectral Density (PSD) matrix  $\mathbf{S}_x(\omega)$ , based on the following expression:

$$\mathbf{S}_x(\omega)\mathbf{\Psi}_x(\omega) = \mathbf{\Psi}_x(\omega)\mathbf{\Lambda}_x(\omega) \Rightarrow \mathbf{S}_x(\omega) = \mathbf{\Psi}_x(\omega)\mathbf{\Lambda}_x(\omega)\mathbf{\Psi}_x^H(\omega) \tag{1}$$

where  $\mathbf{\Lambda}_x(\omega)$  is a diagonal matrix containing nonnegative eigenvalues in decreasing order and  $\mathbf{\Psi}_x(\omega)$  is a complex matrix consisting of mutually orthogonal eigenvectors, being  $\mathbf{\Psi}_x^H(\omega)$  its conjugate transpose. The order of the matrix depends on the number of measured nodal response processes. In detail, each eigenvalue  $\lambda_k(\omega)$  features the average energy distribution of a certain vibration mode over the frequency domain and its local maxima coincide with the eigenfrequencies of the system; whereas each eigenvector  $\mathbf{\Psi}_k(\omega)$  is an estimation of the mode shape corresponding to a certain eigenvalue. Both eigen-parameters are damage-sensitive and play a crucial role for damage identification purposes: eigenvalues changes allow to detect the presence of damage as they are frequency-dependent features, and eigenvectors changes provide spatial information about the damage position as they are coordinate-dependent features [8]. The combination of both parameters is therefore necessary to achieve an accurate damage identification.

### 2.2. Derivation of the spectral damage index

It has been demonstrated [7-8] that the difference between a reference and a damage multivariate stochastic vector process, e.g.  $\mathbf{X}(t)$  and  $\mathbf{X}^d(t)$ , depends on the eigenvectors and eigenvalues in which the PSD matrix of each process is decomposed. Taking this into account, the following spectral damage index has been defined to localize and qualitatively assess the damage [8]:

$$\Delta\psi = \sum_{k=1}^m \left\| \sum_{j=1}^n \left[ \mathbf{\Psi}_k^d(\omega_j) \cdot \sqrt{\lambda_k^d(\omega_j)} \right] \right\| - \left\| \sum_{j=1}^n \left[ \mathbf{\Psi}_k^u(\omega_j) \cdot \sqrt{\lambda_k^u(\omega_j)} \right] \right\| \tag{2}$$

where  $n$  indicates the frequency range,  $m$  represents the eigenvector number and upper scripts  $d$  and  $u$  stand for damaged and undamaged conditions, respectively. The index  $\Delta\Psi$  in Eq. (2) is based on the sum of the differences between the spectral modes of the damaged and undamaged structural conditions, where the spectral modes are estimated through the amplification of the eigenvectors extracted from the response PSD matrix by the square root of their corresponding eigenvalues ( $\Psi_k^d(\omega_j)\sqrt{\lambda_k^d(\omega_j)}$ ). If no damage occurs in the structure, the index  $\Delta\Psi$  in Eq. (2) is equal to zero since  $\Psi_k^d(\omega_j) = \Psi_k^u(\omega_j)$  and  $\lambda_k^d(\omega_j) = \lambda_k^u(\omega_j)$  for any  $k$  and  $j$ . On the contrary, if damage occurs, the index  $\Delta\Psi$  will be different than zero and will result in a vector of scalars (each one associated with a measured DOF) whose magnitude enables to identify the damage position in the system and to give a qualitative estimate of the damage size. For a thorough description of the spectral formulation the reader is referred to [7-8]. The numerical validation and experimental application described in the next sections will better illustrate the proposed approach.

### 3. Numerical simulation and validation

#### 3.1. Description of the numerical model

The case study chosen to validate the spectral method is the Z24 Bridge, a three-span pre-stressed concrete bridge (Fig. 1a) located in Switzerland that was progressively damaged in order to study its dynamic response before being destroyed. A full description of the experimental campaign as well as the induced damage scenarios can be found elsewhere [9]. The damage scenario considered in this work refers to the settlement of the right supporting pier which caused several cracks in the bridge girder above. A beam-like model representing the bridge was built in DIANA software [10] and calibrated according to the dynamic features extracted from experimental data (Fig. 1b). To replicate the settlement of the right pier, damage was simulated by a 60% reduction of the Young's modulus in the beam elements of the girder above this support (Fig. 1c). Four types of input signals were generated and applied to the bridge in order to collect its acceleration response for both reference and damage configurations. Excitation and measuring points are indicated in Fig. 1. Due to space limitations, only the results from two excitation sources, i.e. impulse and ramp force, are presented next. A thorough description of the numerical validation is presented in [7].

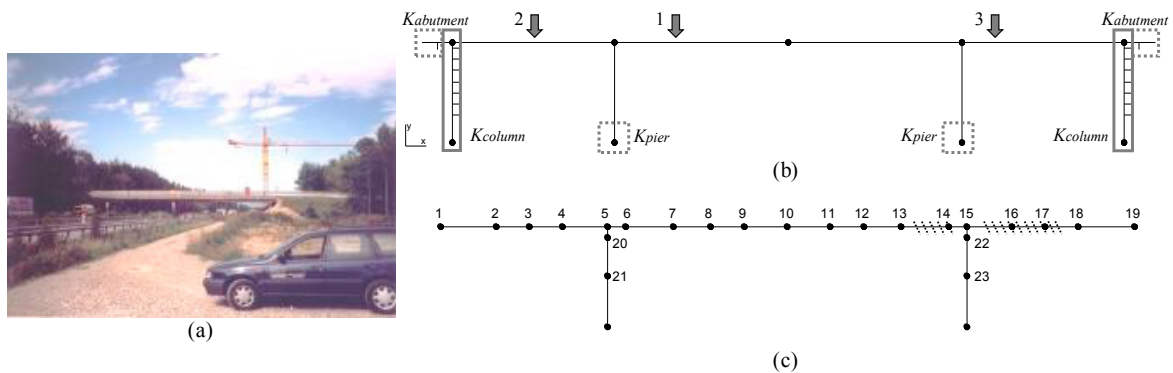


Fig. 1. Z24 Bridge: (a) overview of the structure [9]; (b) FE beam model (1, 2 and 3 are the excitation points); (c) schematization of the simulated damage scenario (dot lines) and indication of the measuring points.

#### 3.2. Validation of the spectral-based damage identification method

With a sampling frequency of 100 Hz and a measurement time of 80s (7999 data points per channel), 23 nodal response processes are recorded and used for the spectral damage identification. As preliminary analyses revealed that the selected damage scenario mainly influences vertical bending modes, only the output signals in vertical direction ( $y$ ) are exploited. A [23x23] PSD matrix is built and decomposed according to the procedure described in Section 2. The extracted eigenvalues are then plotted for the estimation of the eigenfrequencies of the system. The results for the first three modes of vibration are compared in Table 1.

Table 1. Frequency changes between undamaged and damaged configurations for either excitation.

Mode	$f_{UND}$ [Hz]		$f_{DAM}$ [Hz]		Frequency Difference [%]	
	Impulse	Ramp	Impulse	Ramp	Impulse	Ramp
1	3.89	3.89	3.67	3.67	- 5.66	- 5.66
2	4.93	4.93	4.81	4.81	- 2.43	- 2.43
3	10.62	10.49	10.38	10.23	- 2.26	- 2.48

The frequency change between sound and damaged conditions comes from the stiffness degradation of the bridge girder, numerically simulated by reducing the Young's modulus. Indeed, the eigenvalues shifts allow to qualitatively detect the presence of damage, but do not provide any information about its position. To pinpoint the damage, the spectral index in Eq. (2) is computed for both types of excitation. The results are displayed in Fig. 2, where the number of each bar coincides with a measurement point (see Fig. 1c) while the size of each bar  $\Delta\psi$  gives a qualitative estimate of the damage size affecting that particular node or the area close by. For the impulse case (excitation points 1-2), the spectral index accurately identifies the damage in the nodes corresponding to the areas in which Young's modulus has been reduced (nodes 13-14, 16-18), although higher peaks stick out towards the right side (nodes 16-18). As expected, no damage affects node 15 since the girder above the settled pier starts cracking at a certain distance from the joint and the Young's modulus was reduced on the base of this damage scenario. Yet, false positives are detected when the structure is excited close to the damage area (excitation point 3). For the ramp force case, the algorithm plotting provides peaks consistent with the ones obtained from impulse data. False positives are again identified when the system is excited nearby the damaged region (excitation point 3). Notwithstanding, it is worth noting that, even though the spectral damage localization index may yield false positives, indicating the presence of damage where none exists, it does not yield false negatives which would indicate the absence of dangerous situations when damage exists.

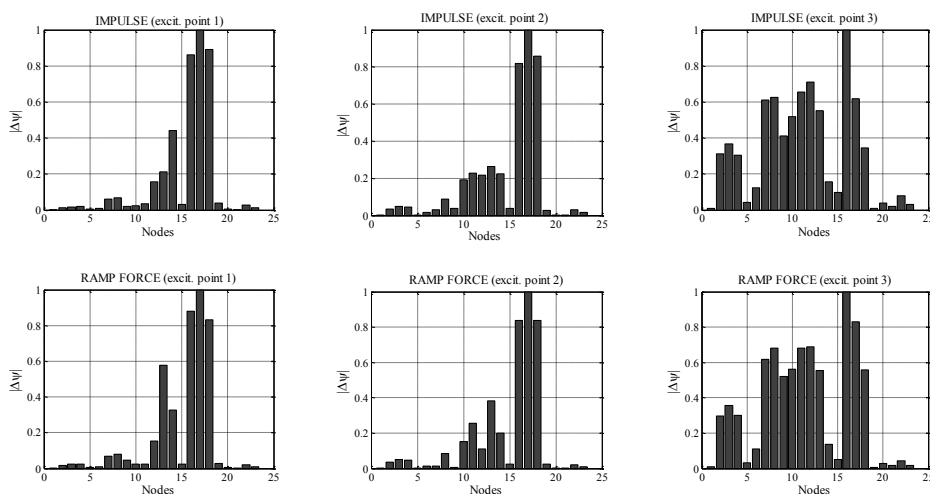


Fig. 2. Damage localization by the spectral index: comparison of the results for different excitation sources.

#### 4. Experimental application to a masonry arch

##### 4.1. Description of the experimental campaign

In this section, benchmark experimental data [11] are used for a direct verification of the spectral algorithm. Object of the experimental campaign was an ancient masonry arch replica built with low compressive strength clay bricks and low quality mortar joints, and characterized by a semi-circular shape with a span of 1.50 m, a width equals to 0.45 m and a thickness of 0.05 m (Fig. 3). The arch was damaged by statically increasing loads, applied at a quarter of the span (Fig. 3a), inducing eight different Damage Scenarios (DS<sub>I</sub> to DS<sub>VIII</sub>). Four cracks appeared during the testing, but

they only became visible in the loading range of the last damage scenario, i.e. DS<sub>VIII</sub>, with the exception of the first crack that was detected during the loading branch of DS<sub>VI</sub>. The resulting crack pattern ( $c_1$  to  $c_4$ ) is presented in Fig. 3. After each load stage, the dynamic response of the system was measured in order to follow the evolution of the modal properties along the testing and to check the stiffness degradation of the arch with increasing damage. An impact hammer of 2.5 kg was used to randomly excite the structure. The nodal processes were acquired by 22 accelerometers evenly distributed along either edge of the arch, measuring the response in both normal and tangential directions, as well as 11 strain gauges placed along the middle line of the arch. The location of the measuring points is schematized in Fig. 3b. A sampling frequency of 500 Hz and a minimum measuring time of 60 s were fixed, resulting in 30.000 data points per channel. Detailed information about the overall experimental campaign are given in [11].

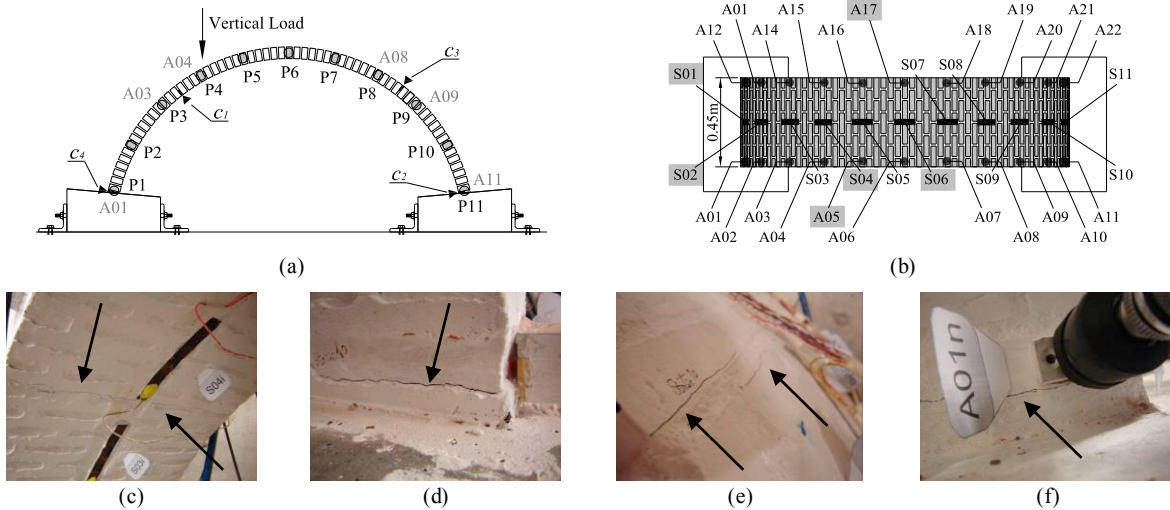


Fig. 3. The masonry arch: (a) schematization of the static tests and relevant crack pattern; (b) location of the measuring points for the dynamic tests ( $A_i$  denote accelerometers and  $S_i$  strain gauges; reference sensors are indicated in grey boxes); (c)-(f) photographic survey of the cracks (in order  $c_1$  to  $c_4$ ) after the last static test.

#### 4.2. Spectral damage analysis of the arch

To perform the spectral damage analysis of the arch, three square PSD matrices are built for each scenario: two  $[22 \times 22]$  matrices from acceleration responses in both normal ( $z$ ) and tangential ( $x$ ) direction and a  $[11 \times 11]$  matrix from strain measurements. Each matrix is then decomposed for the extraction of damage-sensitive parameters (eigenvalues and eigenvectors). As modal strains allow the direct estimation of modal curvatures, quantities much more sensitive than others to structural damage, the results hereafter presented will only refer to the eigen-parameters estimated from the strain PSD matrix. For a complete description of the spectral damage analysis the reader is referred to [8]. The diagonalization of the matrix with the subsequent eigenvalues analysis enabled the identification of 7 vibration modes and the observation of eigenfrequency shifts over all consecutive scenarios, thereby allowing to qualitatively detect the presence of damage. As the damage increases, the structural stiffness of the arch degrades, resulting in lower frequency values. The results for the main DSs are summarized in Table 2.

Table 2. Eigenfrequencies decrease over the main damage scenarios.

Damage Scenario	Eigenfrequencies [Hz]						
	Mode 1	Mode 2	Mode 3	Mode 4	Mode 5	Mode 6	Mode 7
RS	35.13	66.62	71.21	124.8	140.0	172.9	195.7
DS <sub>v</sub>	33.34	65.03	68.83	123.7	134.7	171.5	192.8
DS <sub>vI</sub>	32.56	64.07	67.54	121.8	134.2	169.7	188.2
DS <sub>vII</sub>	30.53	61.61	64.90	121.4	130.6	164.8	182.1
DS <sub>vIII</sub>	26.66	55.53	61.33	119.2	126.7	150.2	179.7

In order to move from a global to local damage identification, the spectral algorithm is applied, allowing to compare the spectral modes of the arch. The results are displayed in Fig. 4. Since the first crack was experimentally detected during the loading branch of  $DS_{VI}$ ,  $DS_V$  is the first scenario considered in the comparison with the Reference Scenario (RS). As it can be seen, damage is successfully detected in the nodes nearby the observed experimental cracks, namely at positions P1, P4, P8 and P11. Furthermore, three out of four cracks are early identified from  $DS_V$ .

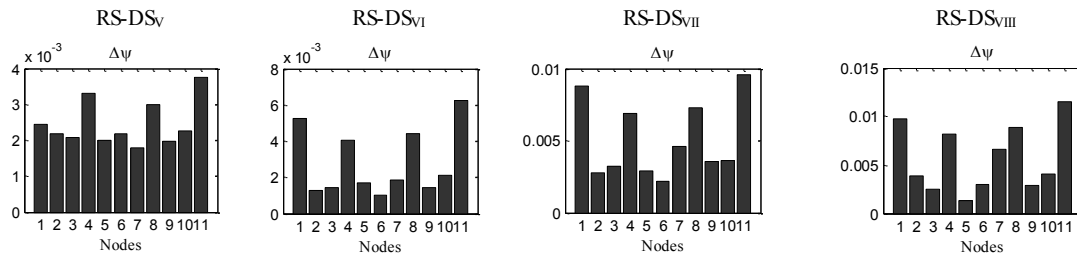


Fig. 4. Results of the spectral damage index: comparison of different DSs with the RS (the number of each bar coincides with a measuring point).

## 5. Conclusions

The paper described a spectral-based method for non-destructive damage identification. Despite the basic assumptions of the formulation are not completely new in literature, in this study the spectral technique is adopted with a new purpose, leading to the definition of a novel damage localization index. As a validation, the technique is applied to a numerical model simulating the behaviour of the Z24 Bridge. Then, the case-study of an old masonry arch replica subjected to increasing damage is presented to evaluate the capability of the method to early detect and locate the cracks. The spectral results proved to be in agreement with both numerical and experimental evidence, confirming the potential of the spectral algorithm as a non-destructive technique for early-stage damage identification.

## Acknowledgements

This work was financed by FEDER funds through the Competitiveness Factors Operational Programme - COMPETE and by national funds through FCT – Foundation for Science and Technology within the scope of the project POCI-01-0145-FEDER-007633. The authors would also like to thank Prof. Dr. Guido De Roeck for sharing his information about the Z24 Bridge.

## References

- [1] A.K. Pandey, M. Biswas, & M.M. Samman, Damage detection from changes in curvature mode shapes. *Journal of Sound and Vibration*, 145(1991) 321–332.
- [2] M.M. Abdel Wahab & G. De Roeck, Damage detection in bridges using modal curvatures: application to a real damage scenario. *Journal of Sound and Vibration*, 226(1999) 217–235.
- [3] J.T. Kim & N. Stubbs, Crack detection in beam-type structures using frequency data. *Journal of Sound and Vibration*, 259(2003) 145–160.
- [4] S. Doebling, C. Farrar, & M. Prime, A summary review of vibration-based damage identification methods. *Shock and vibration digest*, 30(1998) 91–105.
- [5] E. Carden & P. Fanning, Vibration based condition monitoring: a review. *Structural Health Monitoring*, 3(2004) 355–377.
- [6] W. Fan & P. Qiao, Vibration-based damage identification methods: a review and comparative study. *Structural Health Monitoring*, 10(2010) 83–111.
- [7] M.-G. Masciotta, L.F. Ramos, P.B. Lourenço, M. Vasta, G. De Roeck, A Spectrum-driven damage identification technique: application and validation through the numerical simulation of the Z24 Bridge, *Mechanical Systems and Signal Processing*, 70-71 (2016) 578–600.
- [8] M.-G. Masciotta, L.F. Ramos, P.B. Lourenço, M. Vasta, Spectral algorithm for non-destructive damage localisation: Application to an ancient masonry arch model, *Mechanical Systems and Signal Processing*, 84 (2017) 286–307.
- [9] E. Reynders, G. De Roeck, Continuous vibration monitoring and progressive damage testing on the Z24 bridge, in: *Encyclopedia of Structural Health Monitoring*, 2009.
- [10] DIANA, DIANA Finite Elements Analysis - Release 9.4.4, TNO, Netherlands, 2012.
- [11] L.F. Ramos, G. De Roeck, P.B. Lourenço, A. Campos-Costa, Damage identification on arched masonry structures using ambient and random impact vibrations, *Eng. Struct.* 32(2010) 146–162.